Elucidating Dispersion Effects in Perfusion MRI by Means of Dispersion-Compliant Bases

Marco Pizzolato, Timothé Boutelier, Rutger H.J. Fick, Rachid Deriche

ELUCIDATING DISPERSION EFFECTS IN PERFUSION MRI BY MEANS OF DISPERSION-COMPLIANT BASES

Marco Pizzolato[⋆†] *Timothé Boutelier*[‡] *Rutger Fick* [⋆] *Rachid Deriche*[⋆]

[⋆] Athena Project-Team, Inria Sophia Antipolis - Méditerranée, France
[‡] Olea Medical, La Ciotat, France

ABSTRACT

Dispersion effects in perfusion MRI data have a relevant influence on the residue function computed from deconvolution of the measured arterial and tissular concentration time-curves. Their characterization allows reliable estimation of hemodynamic parameters and can reveal pathological tissue conditions. However, the time-delay between the measured concentration time-curves is a confounding factor. We perform deconvolution by means of dispersion-compliant bases, separating the effects of dispersion and delay. In order to characterize dispersion, we introduce shape parameters, such as the dispersion time and index. We propose a new formulation for the dispersed residue function and perform *in silico* experiments that validate the reliability of our approach against the block-circulant Singular Value Decomposition. We successfully apply the approach to stroke MRI data and show that the calculated parameters are coherent with physiological considerations, highlighting the importance of dispersion as an effect to be measured rather than discarded.

***Index Terms*—** perfusion, dispersion, delay, deconvolution, bases

1. INTRODUCTION

The perfusion in the brain can be characterized with Dynamic Susceptibility Contrast Magnetic Resonance Imaging (DSC-MRI). A bolus of paramagnetic agent (PA) is injected into the subject's vascular system and the corresponding concentration time-curve is measured for each voxel. In standard practice, the concentration curve $C_{ts}(t)$ of a tissular voxel is deconvolved with that measured in an arterial area $C_a(t)$ to obtain the residue function $R(t)$ that characterizes the local perfusion. From this, the hemodynamic parameters such as the blood flow (BF) and mean transit time (MTT) are computed. However, the bolus of PA may undergo dispersion after injection, causing the calculated residue function to change according to macro-vascular properties [1]. Dispersion can be present in healthy subjects [2] but it can also be caused by specific pathological conditions, such as the presence of a steno-occlusive disease in the artery [3]. Moreover, dispersion leads to an erroneous quantification of the true perfusion deficit [1]. Indeed, the dispersion of the injected PA bolus causes a modification in the shape of the actual arterial input, which induces a non-monotonic shape in the computed $R(t)$ [1]. This effect is described by an additional unknown convolution kernel - a dispersion kernel - called the vascular transport function (VTF). Another issue in perfusion data processing is the possible presence of a time delay between the tissular concentration time-curve and the measured arterial input. This is a confounding factor for dispersion characterization [4, 5]. Assessment of dispersion is a challenging task but is crucial for decoupling perfusion and macro-vascular influences on the residue function estimated via deconvolution.

Dispersion effects have been tackled by few techniques. One allows to classify voxels where either dispersion or delay is present [4]. The VM+VTF and CPI+VTF [5] aim at quantifying perfusion and dispersion separately, but assume a model for the VTF together with the prior information required for the optimization procedure. The CPI_0 [5] retains a "model-free" nature but fixes the initial value of the residue function to 0, thus preventing an optimal solution in the absence of dispersion. The block-circulant Singular Value Decomposition (oSVD) [6], despite not explicitly aiming at dispersion characterization, allows the reconstruction of dispersed residue functions with no assumptions, and performs comparably to other methods for relative cerebral blood flow estimation in the presence of dispersion [5].

We propose to characterize bolus dispersion in DSC-MRI data without any *a priori* assumption on the residue function and vascular transport function. We perform deconvolution with dispersion-compliant bases [7] obtaining a representation of the residue function which allows the decoupling of time-delay and dispersion effects. We derive an analytic representation of the dispersed residue function, to be used for *in silico* experiments that validate the reliability of the adopted approach against oSVD [6] at different levels of dispersion. We introduce the use of shape parameters, the dispersion time and index, to detect presence and amount of dispersion in the shape of the residue function. We show the effectiveness of the approach with synthetic experiments and on stroke MRI data.

[†]The author expresses his thanks to Olea Medical and to the Provence-Alpes-Côte d'Azur Regional Council for providing grant and support.

2. DISPERSED RESIDUE FUNCTION

According to the indicator-dilution theory [8], the tissular concentration time-curve $C_{ts}(t)$ in a voxel is expressed as the convolution between the arterial input $C_a(t)$ and the unknown residue function $R(t)$, which expresses at each time t the residual amount of PA in the voxel

$$C_{ts}(t) = BF \cdot C_a \otimes R(t) \tag{1}$$

where BF is the unknown cerebral blood flow parameter.

In presence of dispersion, the true arterial input is the result of the convolution of $C_a(t)$ with the vascular transport function $VTF(t)$, which represents the probability density of the transit times t from the arterial measurement location to the voxel where $C_{ts}(t)$ is measured [1]. Therefore eq. (1) becomes

$$\begin{aligned} C_{ts}(t) &= BF \cdot [C_a \otimes VTF(t)] \otimes R(t) \\ &= BF \cdot C_a \otimes [VTF \otimes R(t)]\,(t) \\ &= BF \cdot C_a \otimes R^d(t) \end{aligned} \tag{2}$$

where $R^d(t)$ is the dispersed residue function resulting from the use of the associative property.

In order to perform *in silico* experiments, we derive a formulation of $R^d(t) = VTF \otimes R(t)$. Among the several analytic formulations of $R(t)$, the bi-exponential shows the best *in vivo* fitting performance in normal and Diffusion Positive tissue [9]. It includes a fast and a slow flowing capillary components

$$R_{bi-exp}(t) = f \cdot e^{-\tau_F t} + (1-f) \cdot e^{-\tau_S t} \tag{3}$$

where τ_F and τ_S are the fast and slow time-rates respectively, and f is the relative weight of the fast component. We specialize $R^d(t)$ for the bi-exponential model of eq. (3) in the case of a mono-exponential dispersion kernel $VTF(t) = \beta e^{-\beta t}$ [1, 3, 4] obtaining

$$\begin{aligned} R^d(t) = \frac{-\beta}{(\beta-\tau_F)(\beta-\tau_S)}[(f(\tau_F-\tau_S)+\beta-\tau_F)e^{-\beta t} \\ + f(\tau_S-\beta)e^{-\tau_F t} + (f(\beta-\tau_F)-\beta+\tau_F)e^{-\tau_S t}] \end{aligned} \tag{4}$$

which holds for $\beta > 0$ and, similarly to what observed for the case of the mono-exponential residue function [1], depends on the original mean transit time $MTT = f/\tau_F + (1-f)/\tau_S$.

The dispersion amount induced by $VTF(t)$ on the calculated residue function can be expressed by the vascular mean transit time, which in the case of eq. (4) is $MTT_v = \beta^{-1}$ [1]. Its influence is illustrated in Fig. 1, where the top image shows that dispersion effects increase with MTT_v, being a pure bi-exponential decay for $MTT_v = 0$, whereas the bottom image shows that for a specific value of $MTT_v > 0$ dispersion effects increase also with MTT.

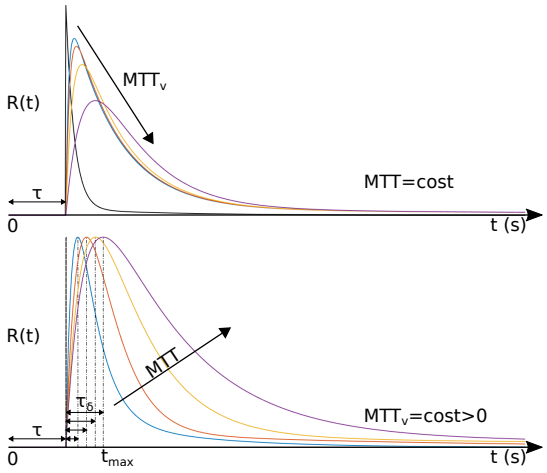

Fig. 1. Influence of dispersion on the calculated residue function and time-delay τ between $C_{ts}(t)$ and $C_a(t)$. Top: the maximum decreases, and the time of the maximum t_{max} and dispersion time τ_δ increase with the vascular mean transit time MTT_v. Bottom: t_{max}, τ_δ increase with MTT (curves are normalized).

We propose to quantify the deviation of the residue function from a purely decaying shape as the difference between the integrals of the decreasing and increasing parts of the curve, normalized by the total area

$$\delta = \left(\int_{t_{max}}^{\infty} R(t)dt - \int_{\tau}^{t_{max}} R(t)dt\right) \Big/ \int_{\tau}^{\infty} R(t)dt \tag{5}$$

where t_{max} is the time of maximum and τ the time-delay as shown in Fig. 1. The dispersion index indicates the absence of dispersion when $\delta = 1$ or its presence when $\delta < 1$. In addition we note that Fig. 1 illustrates that the difference between t_{max} and τ, henceforth called dispersion time $\tau_\delta = t_{max} - \tau$, increases with MTT and MTT_v. We then propose to calculate dispersion time τ_δ and index δ as shape descriptors of the residue function sensitive to the presence and amount of dispersion.

The next section describes the deconvolution strategy to calculate these parameters and the experimental setup to test dispersion characterization reliability *in silico* and *in vivo*.

3. METHOD AND EXPERIMENTAL RESULTS

The detection of dispersion is carried out by deconvolving the measured $C_a(t)$ and $C_{ts}(t)$ while representing the residue function by means of dispersion-compliant bases [7]

$$R(t) = \Theta(t-\tau)\sum_{n=1}^{N}[a_n + b_n(t-\tau)]e^{-\alpha_n(t-\tau)} \tag{6}$$

where N is the maximum basis order and $\Theta(t)$ is the Heaviside step function assuming $\Theta(0) = 1$. The deconvolution

problem is solved linearly for a_n, b_n subject to $a_n, b_n \geq 0$ to avoid negative solutions, with α_n estimated *a priori* and τ determined via grid search [7].

We perform *in silico* experiments to test the reliability of the adopted deconvolution strategy against oSVD [6]. The measured arterial input $C_a(t)$ is simulated in range $[0, 90]s$ with time step $\Delta t = 1s$ as a gamma-variate function [1]. The tissular concentration $C_{ts}(t)$ is obtained via eq. (2) using the derived dispersed kernel in eq. (4) when $\beta > 0$. Gaussian noise with zero mean is added to obtain concentration time-curves as previously reported [7] with $SNR = 50$ [5]. Deconvolution is performed with the dispersion-compliant bases ($N = 20$) searching for τ in range $[-5, 15]s$ [7] and with oSVD [6]. The effective blood flow BF^* is obtained as the maximum value of the estimated residue function $R(t)$, the blood volume BV as the ratio between the time integrals of $C_{ts}(t)$ and $C_a(t)$, and the mean transit time as the ratio $MTT^* = BV/BF^*$. Results are studied as dispersion effects increase for increasing values of MTT_v, assuming no dispersion for $MTT_v = 0$, i.e., data is generated with eq. (3). We simulate the concentration curves 100 times for each combination of dispersion, $MTT_v \in [0 : 1 : 10]s$, delay $\tau \in [-5 : 1 : 5]s$, original value of blood flow, $BF \in [20 : 10 : 60]ml/100g/min$ with blood volume $BV \approx 2\%$ and original mean transit time $MTT \approx 4s$ ($\tau_F = 0.34$, $\tau_S = 0.025$, $f = 0.97$). Results for $\tau = 2s$ and original $BF = 30ml/100g/min$ are shown in the left column of Fig. 2 and mean relative or absolute errors among all the tested combinations are shown in the right column. We note that deconvolution via dispersion-compliant bases results in more accurate estimates than oSVD. The mean relative errors on BF^* estimates are lower than 20% and uncorrelated with the underlying amount of dispersion (MTT_v). As in the case of oSVD, the performance in estimating MTT^* ameliorates as dispersion increases with an improved accuracy. The mean absolute precision on t_{max} always falls below the sampling time $\Delta t = 1s$ and below $2s$ for τ_δ, as depicted from the green bars in Fig. 2, allowing for dispersion time estimation.

We then applied the compared techniques on $256 \times 256 \times 15$ stroke MRI data, $\Delta t = 1.5s$. The techniques' setups are identical to those of *in silico* experiments. We compute the hemodynamic parameters BF^*, BV and MTT^* and remove large vessels and cerebrospinal fluid (CSF) from the results by setting voxels with $BV > 3\%$ to zero. The data reveals an infarcted region in the right hemisphere and iso-perfused tissue. We report the maps of t_{max} in Fig. 3 where oSVD results confirm the overestimation tendency shown in the last row of Fig. 2, particularly in the infarcted region. Moreover, our approach accounts for both the contribution of the time-delay τ and dispersion time τ_δ which are shown in the top row of Fig. 4. Indeed, the dispersion-compliant bases encompass delayed and dispersed shapes allowing to distinguish between the two different contributions. Although the infarcted region is distinguishable in both the t_{max} and τ maps, the proposed

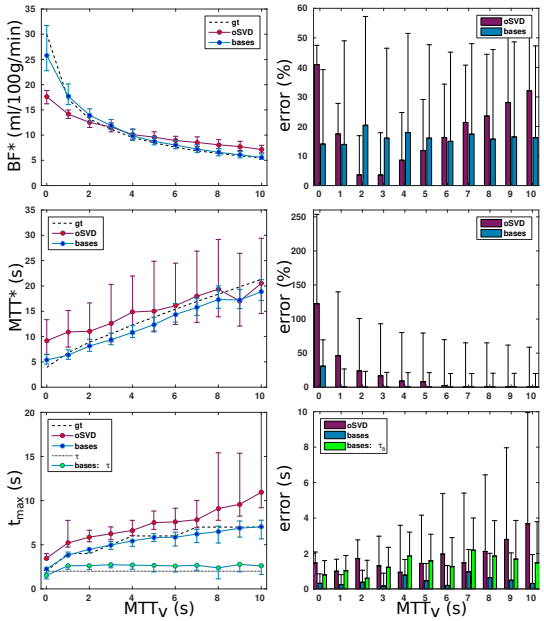

Fig. 2. Estimated (*effective) hemodynamic parameters for $\tau = 2s, BF = 30\,ml/100g/min$ (left column), and overall errors (right column) as dispersion increases according to the vascular mean transit time MTT_v ($SNR = 50$).

dispersion time τ_δ map improves the contrast between the inside and the outside of the infarcted region itself. The map of the dispersion index proposed in eq. (5) is shown in the bottom left corner of Fig. 4. Non-dispersed regions are colored in red ($\delta = 1$), whereas green and blue regions denote moderate and high dispersion respectively. We distinguish two areas within the infarcted region: an upper area mainly characterized by the absence of dispersion, and a lower one dominated by high dispersion (blue color). Moderately dispersed shapes dominate the iso-perfused region which may be caused by natural dispersion effects in the data [2] and noise effects. The dispersion index δ is a relative shape parameter since it characterizes the residue function regardless of its actual size. In order to understand the actual spread of the dispersed residue function, it is interesting to relate its δ value with its measure of the aperture given by the MTT^*. We show the correlation term $\rho_{1-\delta,MTT} = (1-\delta)MTT^*/MTT^*_{max}$ in the bottom right corner of Fig. 4. As expected this map highly correlates with the above dispersion time map τ_δ, $[r \approx 0.95, p < 0.001]$. Indeed, as previously described and illustrated in Fig. 1, the dispersion time depends on both dispersion effects - MTT_v and its influence on δ - and the mean transit time. We further note how both the τ_δ and $\rho_{1-\delta,MTT}$ maps are insensitive to regions where no dispersion is detected - the red areas in the δ map - being non-zero only in complementary regions.

Overall our approach allows low relative error of BF^*, MTT^* estimates, sub-second precision for t_{max}, and reliable estimation of delay τ and dispersion time τ_δ regardless

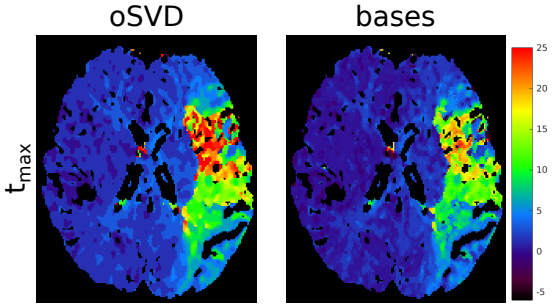

Fig. 3. The time of the maximum t_{max} (s) of the residue function $R(t)$ calculated via oSVD, and dispersion-compliant bases: these reduce overestimation as shown in Fig. 2.

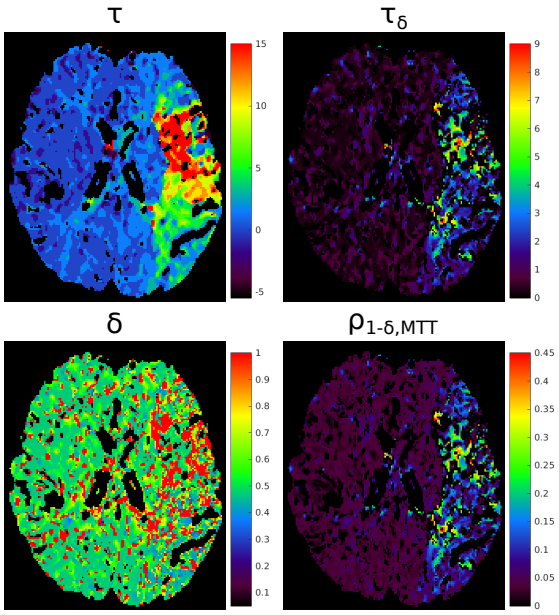

Fig. 4. Maps obtained with dispersion-compliant bases. Time-delay τ (s) and the proposed dispersion time τ_δ (s), dispersion index δ and its correlation with MTT^*, $\rho_{1-\delta,MTT}$.

the amount of dispersion. Furthermore, the proposed index δ provides new insights on dispersion, and its correlation with MTT^* is consistent with τ_δ.

4. CONCLUSION

Dispersion is a phenomenon that can be present in perfusion-weighted data and its characterization is fundamental to assess the reliability of perfusion-related estimates while potentially revealing pathological conditions [4]. In this work we propose a way of characterizing dispersion effects *in vivo* without making any assumption on the dispersion kernel. This is achieved by introducing shape parameters, such as the dispersion time and index, that are calculated on the residue function estimated via deconvolution by means of dispersion-compliant bases. The approach outperforms oSVD and yields reliable estimates specially when the underlying residue function has a dispersed shape, such as in the case of the derived formulation. Results on stroke MRI data confirm *in vivo* the influence of the mean transit time on the dispersed shape, showing consistency with the estimated dispersion time and index. The dispersion time is useful in the delimitation of the infarcted area whereas the dispersion index gives new insights on the shape of the residue function. The proposed strategy allows to decouple dispersion effects from the confounding effect of the delay. This opens for dispersion characterization, thus providing a better understanding of the tissue perfusion and vascular dynamic.

5. REFERENCES

[1] Calamante et al., "Delay and dispersion effects in dynamic susceptibility contrast MRI: simulations using singular value decomposition," *Magn Reson Med*, vol. 44(3), pp. 466–473, 2000.

[2] Østergaard et al., "Cerebral blood flow measurements by magnetic resonance imaging bolus tracking: comparison with $[^{15}o]h_2o$ positron emission tomography in humans," *J Cerebr Blood F Met*, vol. 18(9), pp. 935–940, 1998.

[3] Calamante et al., "Estimation of bolus dispersion effects in perfusion MRI using image-based computational fluid dynamics," *NeuroImage*, vol. 19, pp. 341–353, 2003.

[4] Willats et al., "Improved deconvolution of perfusion MRI data in the presence of bolus delay and dispersion," *Magn Reson Med*, vol. 56, pp. 146–156, 2006.

[5] Mehndiratta et al., "Modeling and correction of bolus dispersion effects in dynamic susceptibility contrast MRI: Dispersion correction with cpi in DSC–MRI," *Magn Reson Med*, vol. 72, pp. 1762–1774, 2014.

[6] Wu et al., "Tracer arrival timinginsensitive technique for estimating flow in MR perfusionweighted imaging using singular value decomposition with a blockcirculant deconvolution matrix," *Magn Reson Med*, vol. 50(1), pp. 164–174, 2003.

[7] Pizzolato et al., "Perfusion MRI deconvolution with delay estimation and non-negativity constraints," in *12th International Symposium on Biomedical Imaging (ISBI)*. IEEE, 2015, pp. 1073–1076.

[8] Meier et al., "On the theory of the indicator-dilution method for measurement of blood flow and volume," *J Appl Physiol*, vol. 6(12), pp. 731–744, 1954.

[9] Mehndiratta et al., "Modeling the residue function in DSC-MRI simulations: Analytical approximation to in vivo data," *Magn Reson Med*, vol. 72, pp. 1486–1491, 2014.